Possible Pathways to Producing Rapid Millimeter Accuracy Normal Points

John J. Degnan

2019 ILRS Technical Workshop

Session 1

Stuttgart, Germany

October 21, 2019

Overview

The Global Geodetic Observing System (GGOS) goal of SLR normal points accurate to 1 mm, in addition to a growing list of client satellites, places challenging new demands on the ILRS Network as well as the space segment, which must simultaneously provide adequate array cross-section and minimal pulse spreading. This presentation summarizes and updates options presented by the author in three recent workshops including:

1. The generation of Probability Distribution Functions (PDFs) for returning photons which depend on laser pulsewidth, pulse spreading by the satellite array, detector response, and event timer jitter (Degnan, Canberra 2018).
2. Rapid and accurate determination of the PDF Centroid in generating mm accuracy normal points (Degnan, Riga 2017 and Canberra 2018).
3. Spaceborne retroreflector array designs that provide narrow and highly uniform responses independent of the laser “attack angle” in both elevation and azimuth while simultaneously providing a total optical cross-section appropriate for the operational altitude (Degnan, Potsdam, 2016)

Current Sources of Range Bias

- Optical and electronic delays within the SLR system are usually calibrated by ranging to a single retroreflector placed a known distance from the telescope “invariant point”, defined as the intersection of the telescope elevation and azimuth axes. The PDF of the start channel/instrument is well-mapped by ranging to a single cube calibration target which has a delta-function impulse response.
- Pulse time-of-flight measurements in both legacy multiphoton and newer kHz single photon systems currently rely on threshold detection of the start and stop pulses, where changes in signal amplitude can result in range bias.
- In legacy multiphoton systems, amplitude variations in the start channel are generally quite small and large variations in the stop channel have been greatly reduced through the use of Constant Fraction Discriminators (CFDs).
- True single photon sensitive kHz systems are subject to “first photon range bias” as the received signal strength increases. As a result, they are often operated with return rates of 10% or less to greatly favor single photon returns. The result is a “bias free” range measurement but the larger variance Probability Distribution Function (PDF) requires longer time intervals to achieve a 1 mm Normal Point (NP) This further reduces the number of satellites tracked and extends the length of the satellite arc that the NP represents.
- Nevertheless, in both types of system, the PDFs for photon events in the start and stop channels are different since the satellite signature affects only the PDF of the stop channel. Thus, a range bias in the normal point can result unless the start and stop times are determined by the centroids of the distributions rather than a simple threshold crossing.

Central Limit Theorem (CLT)

If two or more photons are sampled per pulse, the CLT tells us that, on average, the mean of n samples is equal to the mean of the parent distribution, t_c. Thus, no bias is introduced by the multiphoton measurement. As the mean number of photons per pulse increases (n>15), the PDF distribution becomes highly Gaussian in shape, i.e. a “normal” distribution. For an arbitrary distribution of single photon events, one can prove the following for the mean and variance of the n-photon distribution:

n-photon mean

$$\left\langle \frac{1}{n}\sum_{i=1}^{n} t_i \right\rangle = \frac{1}{n}\sum_{i=1}^{n}\langle t_i \rangle = \frac{1}{n} n t_c = t_c$$

Therefore the n-photon mean is unbiased

n-photon variance

$$\sigma_n^2 \equiv \left\langle \left(\frac{1}{n}\sum_{i=1}^{n} t_i\right)\left(\frac{1}{n}\sum_{i'=1}^{n} t_{i'}\right)\right\rangle - t_c^2 = \frac{1}{n^2}\left\langle \sum_{i=1}^{n} t_i^2 + \sum_{i=1}^{n} t_i \sum_{i'\neq i}^{n} t_{i'} \right\rangle - t_c^2$$

$$= \frac{1}{n^2}\left[n\langle t^2 \rangle + n(n-1)t_c^2 \right] - t_c^2 = \frac{\langle t^2 \rangle - t_c^2}{n} = \frac{\sigma_1^2}{n}$$

So the n-photon mean has a variance n times smaller than the single photon distribution

Suitable Centroid Detectors

- The detector must be sensitive to single photons and have the ability to record multiple single photon events per pulse on a single anode.
- MCP/PMTs have thousands of microchannels and SiPMTs have hundreds to thousands of individual APDS, separated spatially by a few microns, which are capable of recording multiple single photon events and combining the outputs onto a single anode.
- The finite size of the satellite image in the telescope focal plane ensures that multiple microchannels or SiAPDs are illuminated and can be further blurred if required.
- If the photons coming back from the satellite are grouped too closely together in time to permit the measurement of individual photon arrival times, the individual photons will create an irregular and complex single pulse of varying amplitude out of the anode whose centroid must be determined.
- Fortunately, microwave radar engineers have developed simple circuits to measure the centroid of an irregularly shaped pulse.

Centroid Detector for Radar

SigmaSpace
EXCELLENCE IN AEROSPACE TECHNOLOGY

US Patent #3,906,377 (Sept. 16, 1975)

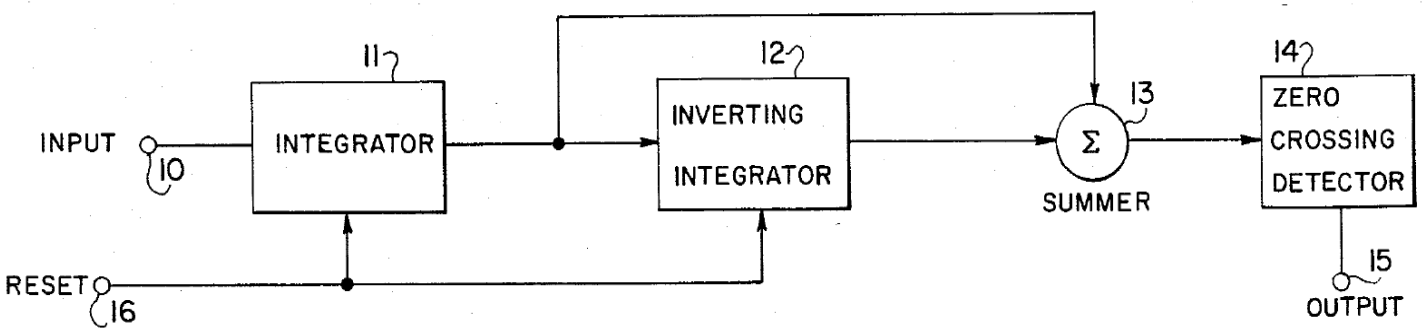

FIG. 1

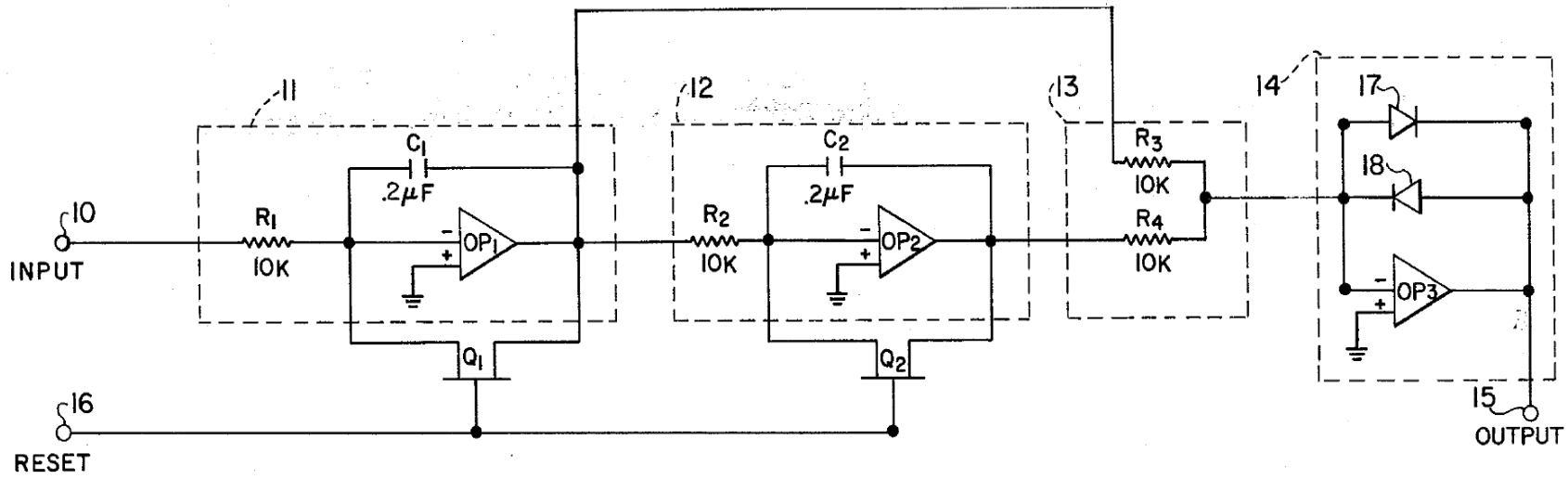

Field Calibration

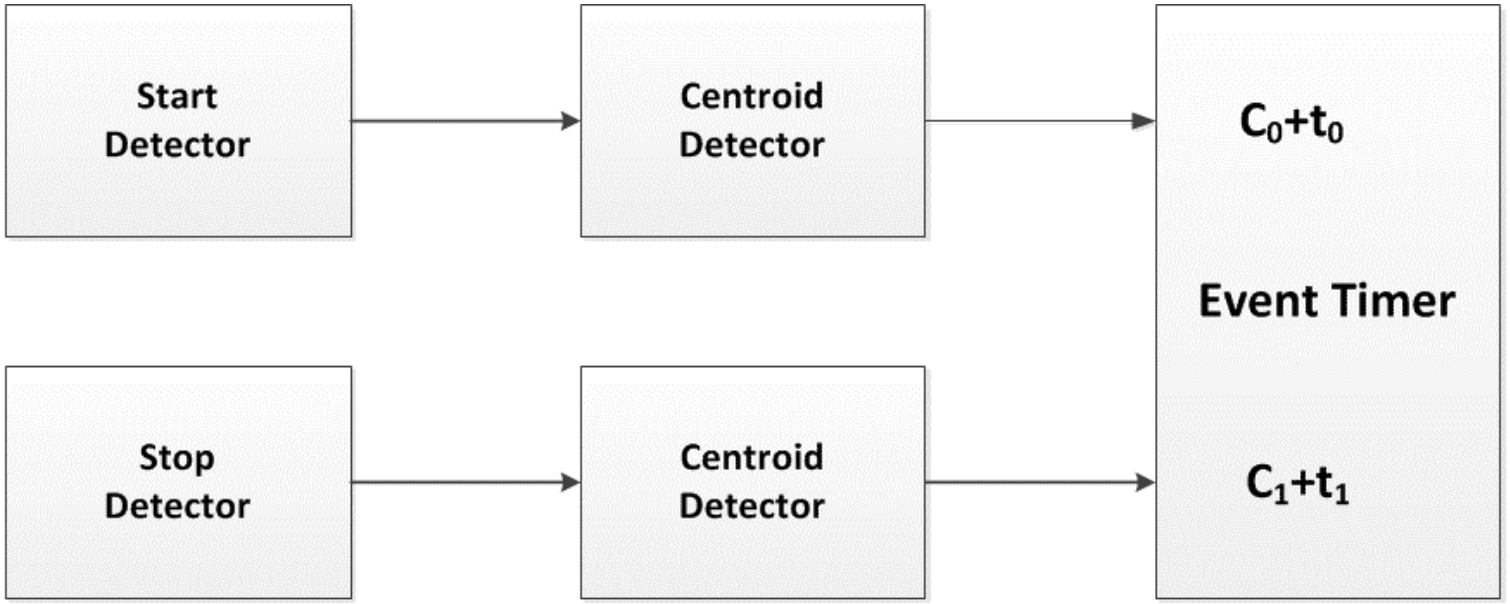

The measured TOF to the calibration target is given by

$$TOF = (C_1 - C_0) + (t_1 - t_0)$$

where t_1 and t_0 are the centroids of the stop and start pulses respectively and $(t_1 - t_0)$ is the actual pulse TOF. The constant $(C_1\text{-}C_0)$ is determined by ranging to a single cube corner at a known distance R_{cal} via the equation

$$(C_1 - C_0) = TOF - 2R_{cal}/c$$

and subtracted from all satellite TOF measurements to obtain a bias free range.

Spherical Satellite Impulse Response*

For a spherical geodetic satellite, the mean impulse response can be described by*

$$I(\tau,\varepsilon,n_{cc},\theta_{\max}) = \sigma_{cc}\frac{N}{2}\sin\theta(\tau,\varepsilon,n_{cc})\left[1-\frac{\theta(\tau,\varepsilon,n_{cc})}{\theta_{\max}}\right]^2$$

where σ_{cc} is the optical cross-section of a single cube corner, N is the number of cube corners uniformly distributed over the spherical surface, n_{cc} is the refractive index of the cube corner, $\varepsilon = n_{cc}L_{cc}/R_s$ is the ratio of the optical length (face to vertex) of an individual cube ($n_{cc}L$) to the satellite radius R_s, $\tau = ct/2R_s$ is a normalized time expressed in units of the roundtrip transit time of the laser pulse from the surface of the satellite to the satellite center of mass and back, θ_{max} is the maximum acceptance angle of the retroreflector from normal incidence. The quantity $\theta(\tau,\varepsilon, n_{cc})$ is obtained by solving the equation

$$\cos\theta(\tau,\varepsilon,n_{cc}) = \frac{1-\tau}{1-\varepsilon\sqrt{1-\frac{1}{n_{cc}^2}+\left(\frac{\cos\theta(\tau,\varepsilon,n_{cc})}{n_{cc}}\right)^2}}$$

as a function of τ. The target PDF $T(t)$, used in computing of λ (t), is $I(\tau,\varepsilon,n_{cc})$ whose integral is normalized to 1.

*** See J. Degnan, "Millimeter Accuracy Satellite Laser Ranging: A Review", Contributions of Space Geodesy to Geodynamics: Technology, D. E. Smith and D. L. Turcotte (Eds.), AGU Geodynamics Series, Volume 25, pp. 133-162**

LAGEOS Impulse Response

The graphs below present the mean impulse response for LAGEOS, i.e. the target PDF $T(t)$ used in the generation of $\lambda(t)$, expressed as a function of $\tau = ct/2R_s$ on the left and distance of the return from the satellite Center of Mass (CoM) on the right. The centroid of the PDF is indicated by the blue dots, i.e. $\tau_c = 0.16$ corresponding to a satellite radius from CoM of ~250.1 mm in good agreement with LAGEOS lab measurements. The total width (zero to zero) of the LAGEOS impulse response is about 70 mm or 468 psec.

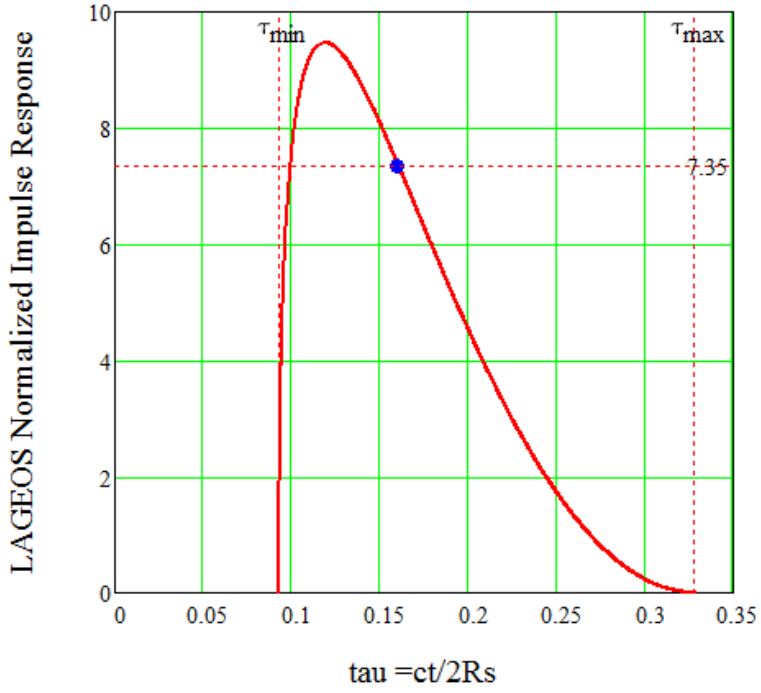

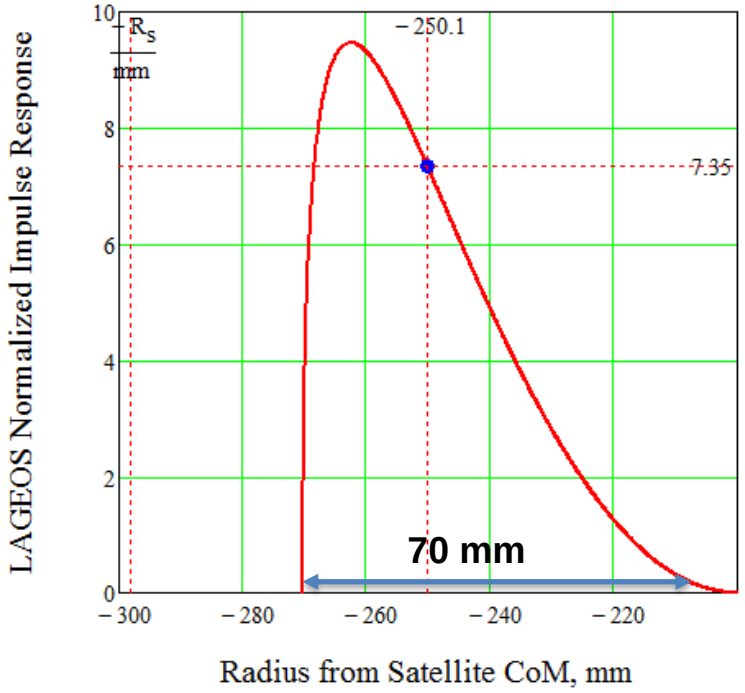

Quasi-Centroid Detection

Unfortunately, to the author's knowledge, a suitable centroid detection circuit has not yet been developed in the subnanosecond pulse optical regime. However, In some of our airborne single photon lidars and most recently in lab tests of SGSLR (see the presentation by Hoffman et al and the poster by Clarke et al), we have improved the range accuracy and stability by recording the times at which the electronic pulse from a single photon event crosses a fixed threshold in both the upward and downward direction. For a broad temporally symmetric pulse, the average would provide the temporal peak (centroid) of the pulse while, for an asymmetric pulse, it would give an imperfect estimate of the pulse centroid (as demonstrated below for the LAGEOS PDF) and the bias magnitude would depend on the choice of threshold. On the other hand, if the instrument PDF was sufficiently narrow to accurately record the arrival times of individual photons, the bias would be largely eliminated

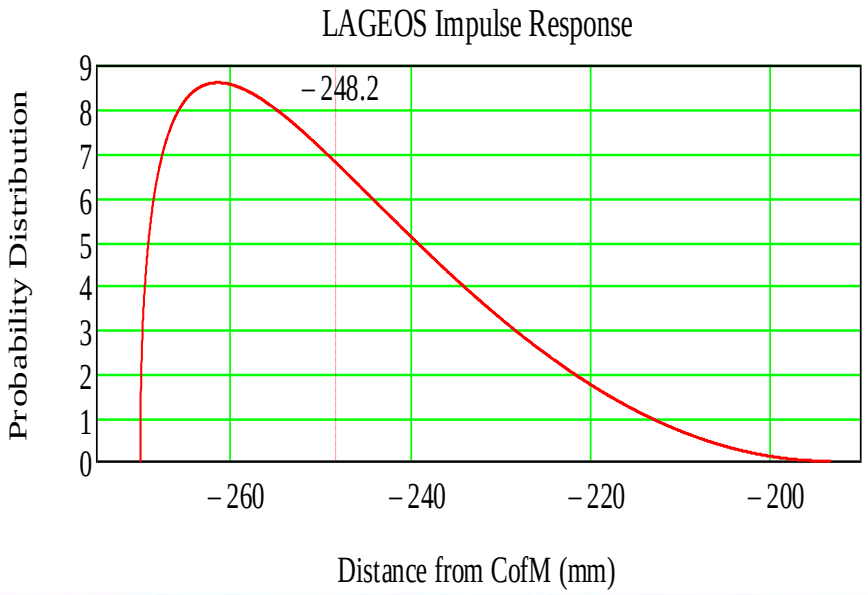

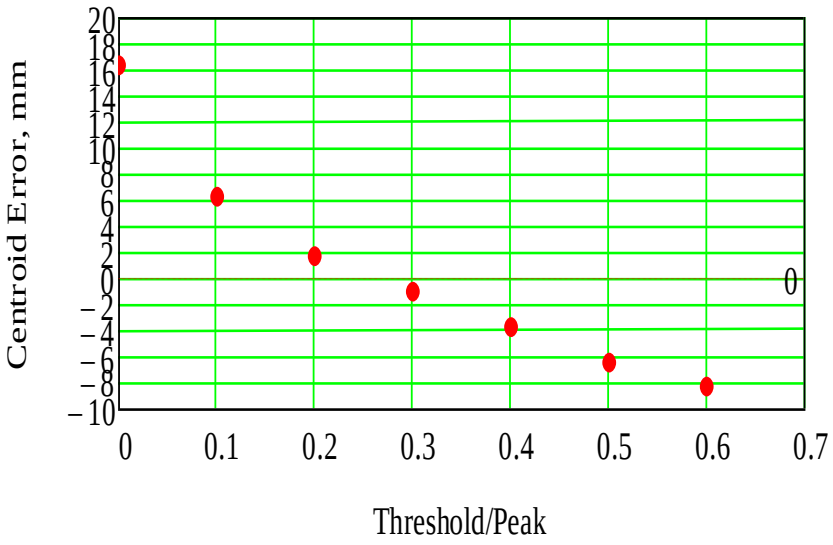

Probability Distribution Function (PDF)

The PDF for the photon time of arrival at the receiver is obtained by convolving the PDFs of the laser (L), the target (T), and the receiver (R), i.e.

$$\lambda(t) = L * T * R$$

Thus, the photoelectrons arriving at the receiver have a PDF given by

$$\lambda(t) = \int_{-\infty}^{t} dt' R(t-t') \int_{-\infty}^{t'} dt'' L(t'') T(t'-t'')$$

which, for a single retro calibration target having a delta function response, reduces to

$$\lambda_c(t) = \int_{-\infty}^{t} dt' R(t-t') \int_{-\infty}^{t'} dt'' L(t'') \delta(t'+\tau_c - t'') = \int_{-\infty}^{t} dt' R(t-t') L(t'+\tau_c)$$

where τ_c is the roundtrip flight time to the target. The instrument PDF due to the laser and receiver, $\lambda_c(t)$, can be measured at the output of the detector with a high speed oscilloscope or, for ultrashort pulses, a sampling scope, but we will now provide an experimental alternative for determining $\lambda_c(t)$.

Detection as a Two State Markov Process

Threshold detection can be treated as a Two State Markov Process with the initial state being "no detection" and the final state being "detection" (if n>0). The time of detection PDF depends on the detection threshold, *T*, the number of photoelectrons detected, *n*, and the n-photon temporal PDF distribution $\lambda(t)$ given by

$$P_n(t) = \frac{1}{1-e^{-n}} a(n,T,t) \exp\left[-\int_{t_0}^{t_f} dt' a(n,T,t') \right]$$

where

$$a(n,T,t) = n\lambda(t) \frac{\left[n\lambda(t) \right]^{T-1}}{(T-1)!} \left\{ \sum_{k=0}^{T-1} \frac{\left[n\lambda(t) \right]^k}{k!} \right\}^{-1}$$

For a single photon detection threshold ($T = 1$) as in kHz SLR systems,

$$a(n,1,t) = n\lambda(t) \quad \text{and} \quad P_n(t) = \frac{\mu_n(t)}{1-e^{-n}} = \frac{1}{1-e^{-n}} n\lambda(t) \exp\left[-n\int_{t_0}^{t} dt' \lambda(t') \right]$$

where $\lambda(t)$ has a non-zero value only in the time interval $t_0 < t < t_f$ and the integral of λ (t) over that interval is equal to 1.

Note: once $\lambda(t) = \mu_1(t)$ is known, the functional form of $\mu_n(t)$ is determined for all values of *n*.

Determining λ(t) Experimentally

The function $\lambda(t)$ can be derived from range data to the calibration target (or even a satellite) by utilizing a low return rate (<10%) such that one is always seeing single photon returns. In this instance, the PDF of the measured ranges should obey the functional form

$$P_1(t) = \frac{\mu_1(t)}{1-e^{-1}} = \frac{1}{1-e^{-1}}\lambda(t)\exp\left[-\int_{t_0}^{t} dt'\,\lambda(t')\right] \qquad \text{where } t_0 \le t \le t_f$$

and t_0 and t_f are defined as the end points of the n=1 detection PDF where $\lambda(t)=0$. The following graph shows the unsmoothed single photon PDF, $P_1(t)$, for NASA's prototype NGSLR station ranging to the calibration target.

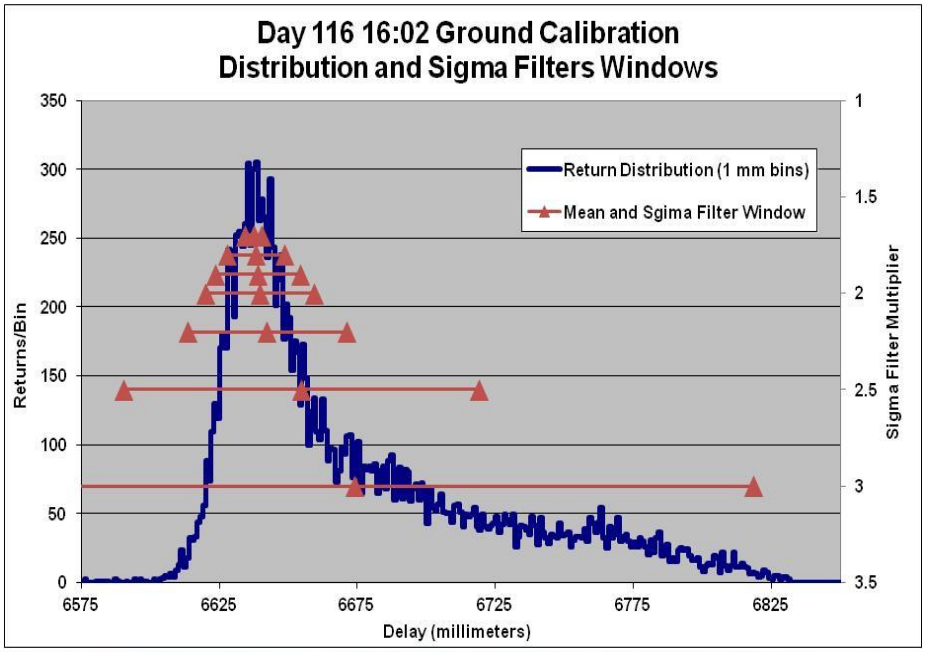

The profile $P_1(t)$ can be smoothed (for example) by: (1) computing the Fourier Transform, (2) applying a bandpass filter to eliminate high frequency noise, and then (3) computing the inverse Fourier transform to provide the function $\mu_1(t)$ in tabulated or functional form. This can then be used to compute $\lambda(t)$ and the n-photon PDFs, $P_n(t)$, for a small range of n values **and correct for signal strength biases in all future measurements to the same target**!

Detection Probability and Normal Point Precision

For a SLR system with a single photon detection threshold, the probability of detecting the satellite signal is

$$P_d(n) = 1 - \exp\left(-n\right)$$

and the number of range measurements contributing to a satellite "normal point" is

$$N = P_d(n) f_L \tau_{np} = \left(1 - e^{-n}\right) f_L \tau_{np}$$

where

f_L = the laser repetition rate = 2 kHz for SGSLR

τ_{np} = the normal point time interval

and the desired normal point precision is equal to

$$\sigma_{np} = \frac{\sigma_n}{\sqrt{N}} = \frac{\sigma_1}{\sqrt{nN}} = \frac{1}{\sqrt{nN}} \sqrt{\sigma_L^2 + \sigma_D^2 + \sigma_{ET}^2 + \sigma_S^2} \approx 1mm$$

where σ_1 is the satellite-dependent , single pulse, single photon range precision obtained from the contributions of the laser (L), detector (D), Event Timer (ET), and Satellite (S). Thus, the integration time required to generate a normal point with precision σ_{np} is given by

$$\tau_{np} = \frac{N}{\left(1 - e^{-n}\right) f_L} = \frac{1}{n\left(1 - e^{-n}\right) f_L} \left(\frac{\sigma_1}{\sigma_{np}}\right)^2 \qquad n \geq 1$$

$$\frac{1}{\left(1 - e^{-n}\right) f_L} \left(\frac{\sigma_1}{\sigma_{np}}\right)^2 \qquad n < 1$$

NGSLR LAGEOS 1mm NP Integration Time vs n

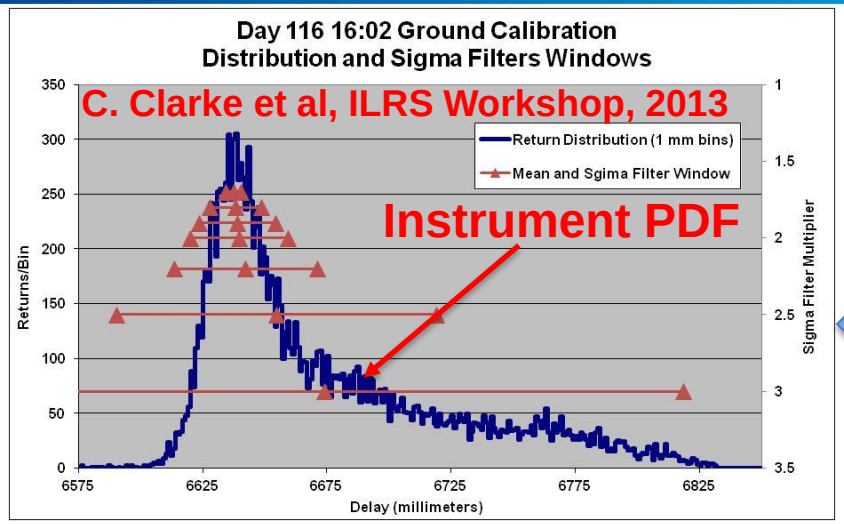

225 mm = 6 σ_{inst}

$$\sigma_{inst} = \sqrt{\sigma_L^2 + \sigma_D^2 + \sigma_{ET}^2} = 37.5mm$$

σ_L = 6.3mm for 50 psec FWHM Laser
σ_D = 36.8 mm for MCP/PMT
σ_{ET} = 3.4 mm for baseline Sigma ET
σ_{inst} = instrument RMS ~ 37.5mm
f_L = laser repetition rate = 2 kHz

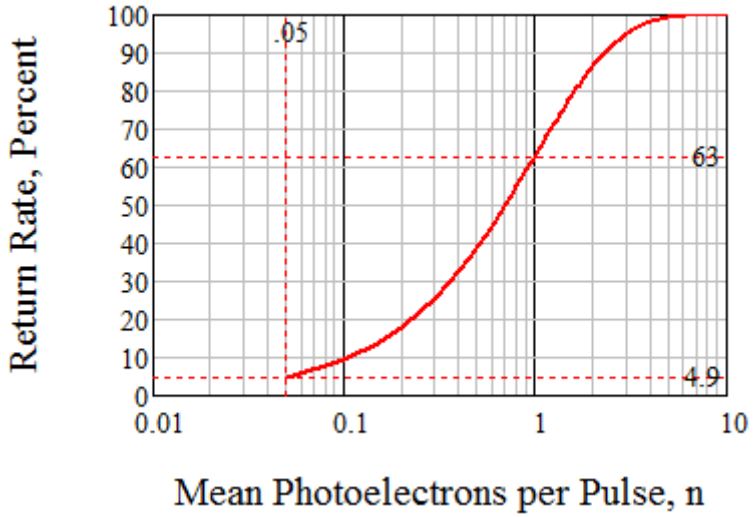

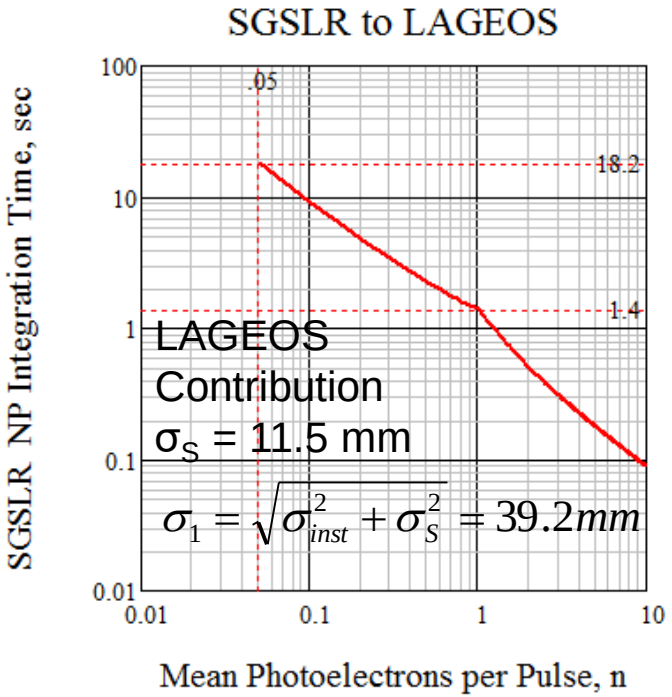

Photoelectron Distribution vs Return Rate

From Poisson statistics, the probability that a given return within the NP consists of *n* photoelectrons when the mean number is η is given by

$$P(n,\eta) = e^{-\eta}\frac{\eta^n}{n!}$$

and the total probability of detecting the signal (i.e. the return rate) is equal to

$$P_D(\eta) = \sum_{n=1}^{\infty} P(n,\eta)$$

$$= e^{-\eta}\sum_{n=1}^{\infty}\frac{\eta^n}{n!} = 1 - e^{-\eta}$$

where the mean signal strength (η) and Return Rate (*RR*) are equal to

$$\eta = \ln\left(\frac{1}{1-P_D}\right)$$

$$RR = P_D(100\%)$$

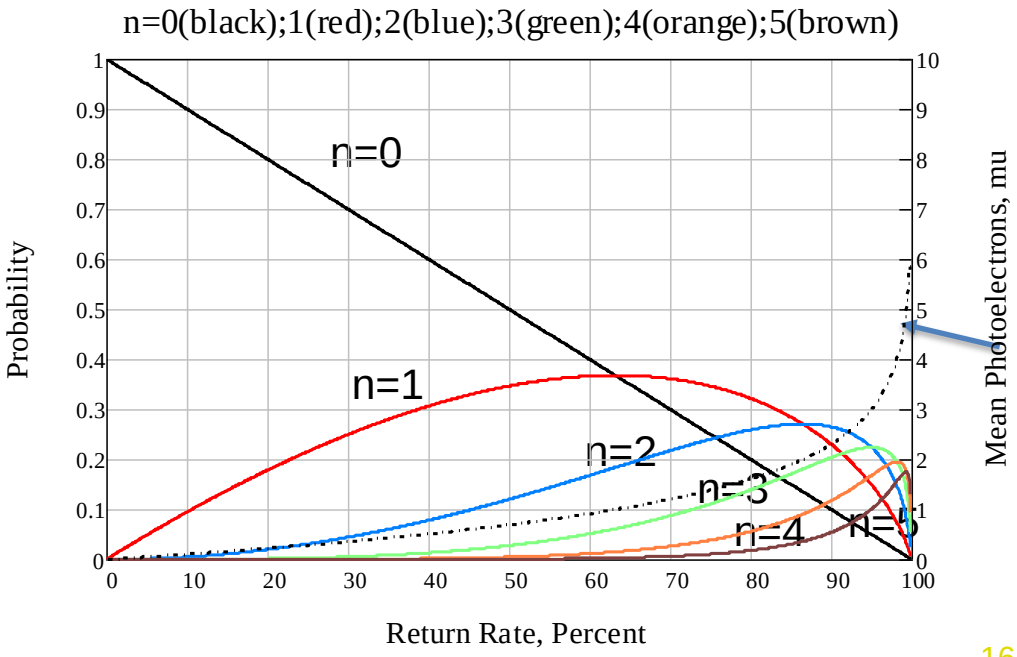

Computing λ(t) from $\mu_1(t)$

We begin by computing $\mu_1(t)$ from the observed single photon PDF $P_1(t)$

$$\mu_1(t) = \left(1 - e^{-1}\right) P_1(t) \equiv \lambda(t) \exp\left[-\int_{t_0}^{t} \lambda(t')dt'\right] = -\frac{d}{dt} \exp\left[-\int_{t_0}^{t} \lambda(t')dt'\right]$$

Integrating both sides of the equation with respect to t yields

$$\exp\left[-\int_{t_0}^{t} \lambda(t')dt'\right] = 1 - \int_{t_0}^{t} \mu_1(t')dt'$$

Computing the logarithm of both sides gives

$$\int_{t_0}^{t} \lambda(t')dt' = \ln\left(\frac{1}{1 - \int_{t_0}^{t} \mu_1(t')dt'}\right)$$

and differentiating both sides with respect to t yields our final result

$$\lambda(t) = \frac{\mu_1(t)}{1 - \int_{t_0}^{t} \mu_1(t')dt'}$$

Detection Centroid for Arbitrary Return Rate

For a normal point generated with multiple values of *n* and having a mean signal strength η, the bias in the photon time of flight is

$$\Delta t(\eta) = \langle t(\eta) \rangle - \langle t_0 \rangle = \sum_{n=1}^{\infty} P(n,\eta) \langle t_n \rangle - \langle t_0 \rangle = e^{-\eta} \sum_{n=1}^{\infty} \frac{\eta^n}{n!} \langle t_n \rangle - \langle t_0 \rangle$$

where the centroid of the PDF for *n* detected photoelectrons is given by

$$\langle t_n \rangle \equiv \int_{t_0}^{t_f} dt t P_n(t) = \frac{1}{1-e^{-n}} \int_{t_0}^{t_f} dt t \mu_n(t) = \frac{n}{1-e^{-n}} \int_{t_0}^{t_f} dt t \lambda(t) \exp\left[-n \int_{t_0}^{t} dt' \lambda(t') \right]$$

which, in the limit as n goes to zero, reduces to the unbiased photon arrival time

$$\langle t_0 \rangle = \int_{t_0}^{t_f} dt t \lambda(t)$$

NGSLR to Calibration Target

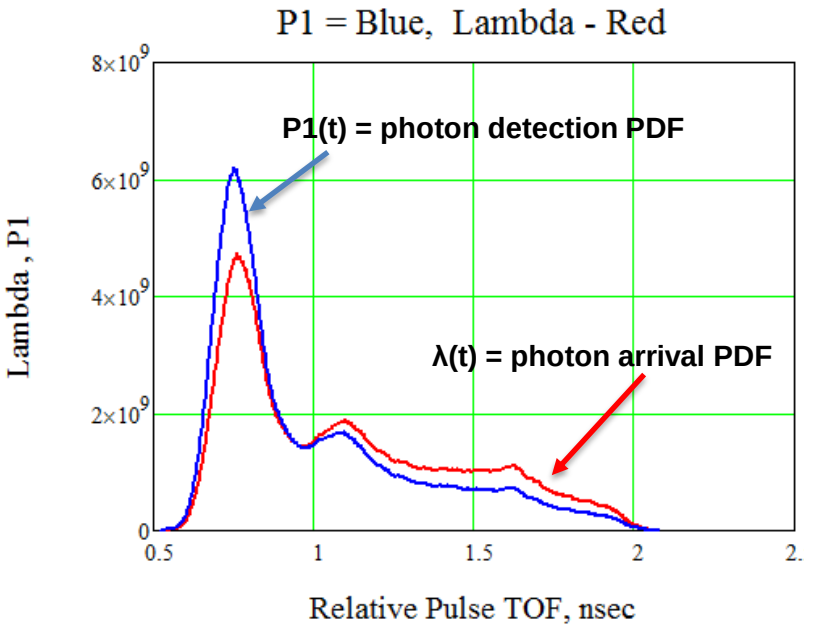

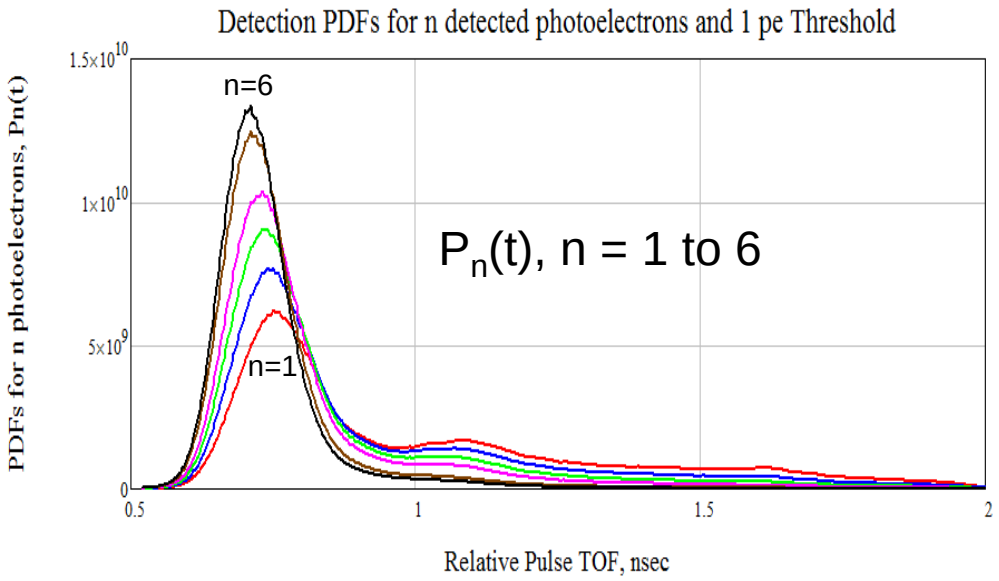

Time and Range Bias vs Number of Detected Photoelectrons (n =0 to 10)

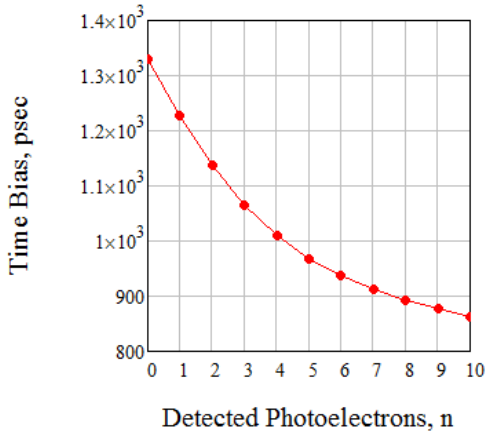

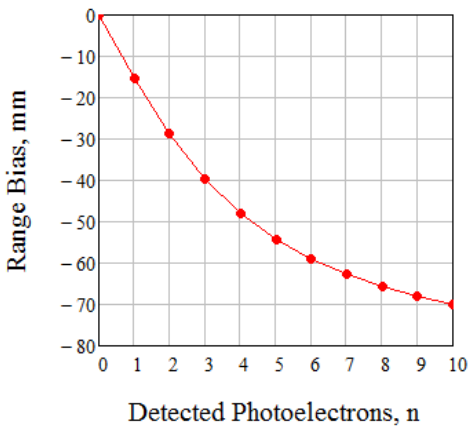

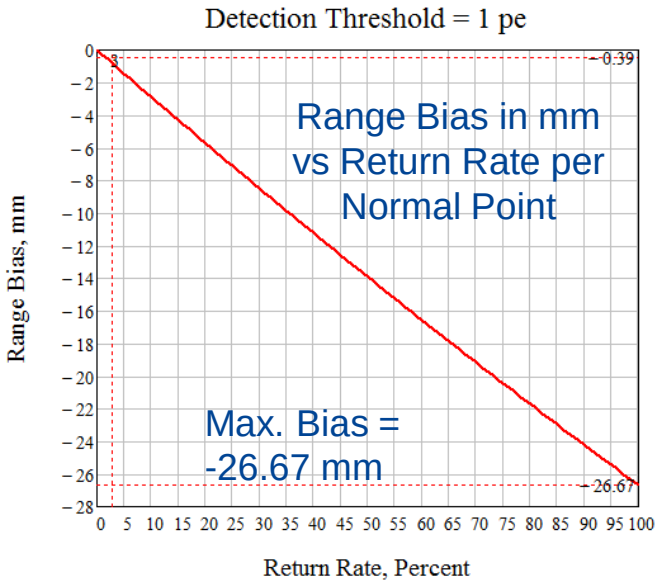

NGSLR Calibration Test
Theory vs Experiment

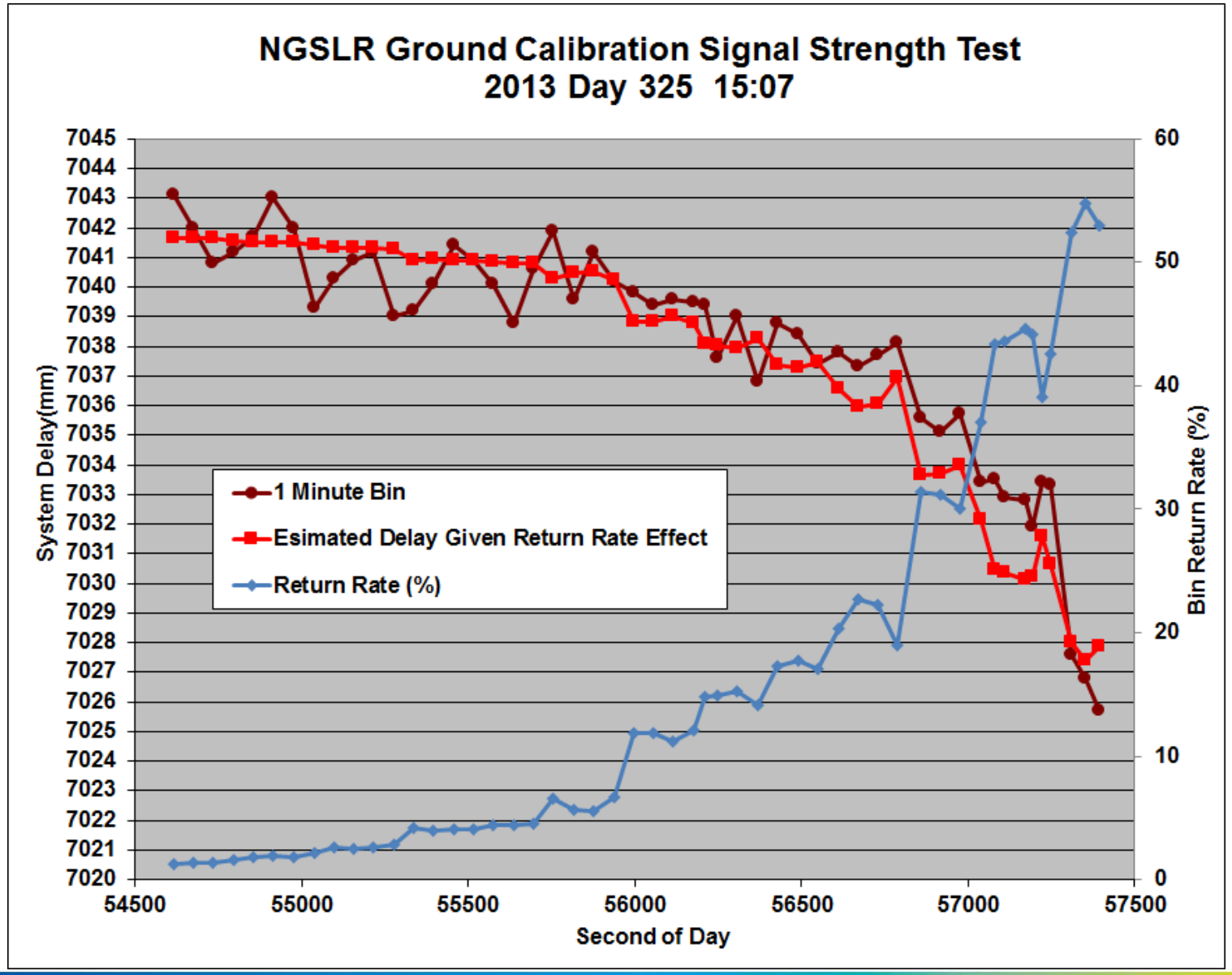

NGSLR to LAGEOS

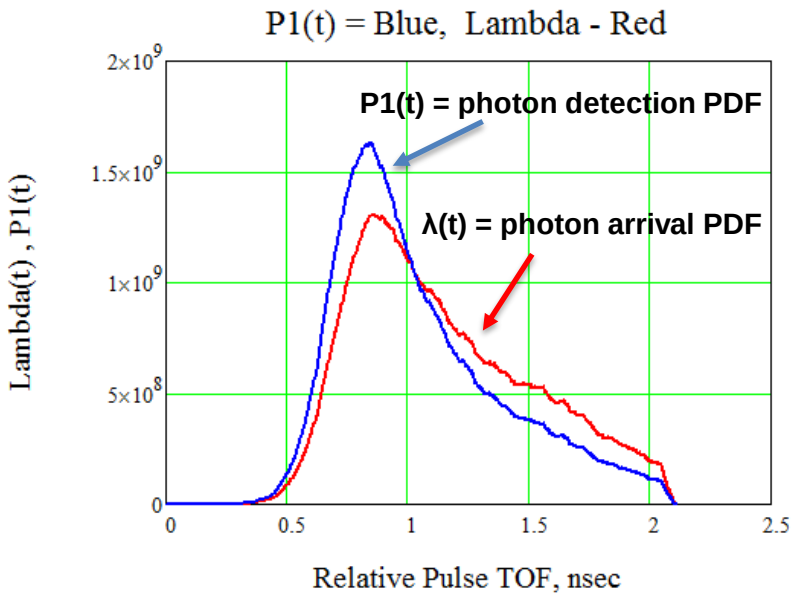

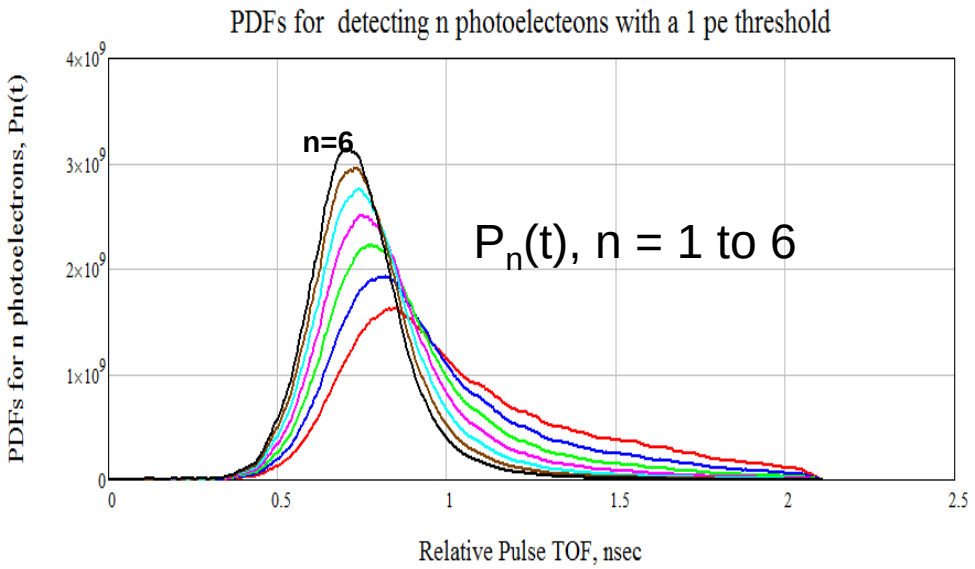

Time and Range Bias vs Number of Detected Photoelectrons (n =0 to 10)

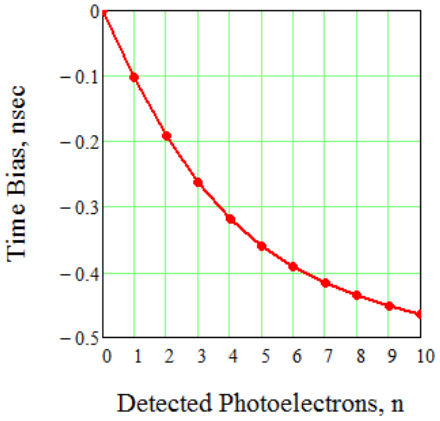

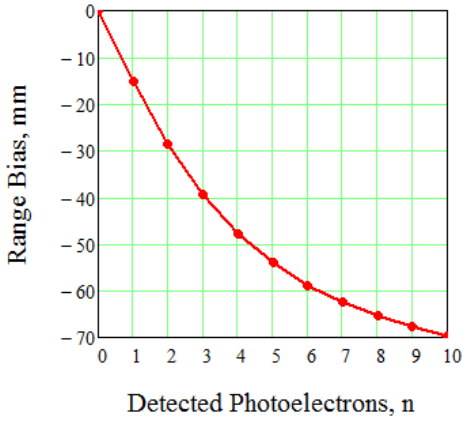

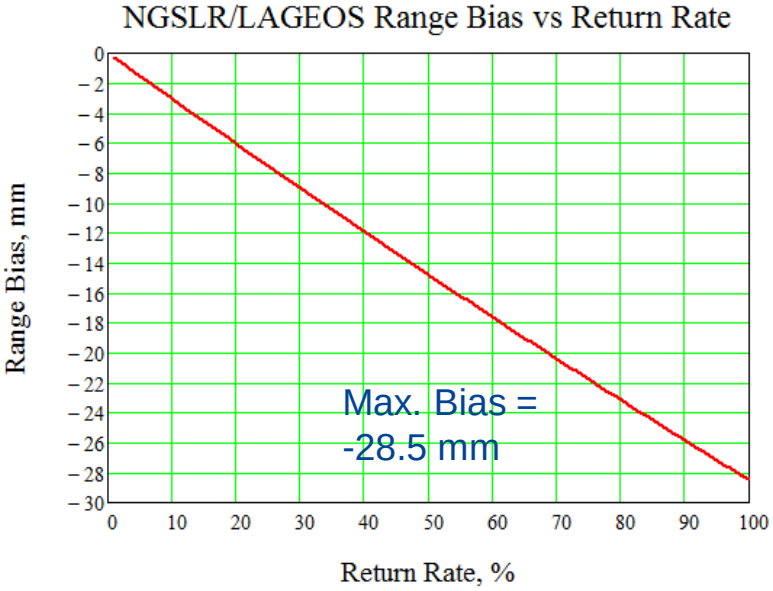

MM ACCURACY GEODETIC SATELLITES

Technical Challenges and Solutions

Challenge: Geodetic satellites (e.g., LAGEOS, Starlette, etc.) are typically in low to medium altitude orbits, and rotate freely in space.
Solution: Spherical satellites permit a quasi-uniform response independent of the laser attack angle.

Challenge: The satellite must present a high enough cross-section, consistent with its maximum range, to support ranging by the entire ILRS network.
Solution: Since velocity aberration limits the size of the individual retroreflectors at lower altitudes, cross-section must be achieved by increasing the number of retroreflectors contributing to the station return. This can be achieved by building larger spheres, which present more surface area able to accommodate a larger number of reflectors, and/or Improving the packing density to increase the number of retros per unit surface area.

Challenge: Reduce the spread in the satellite impulse response to improve range accuracy and precision.
Solution: Since the strength of an individual retro return diminishes as one gets farther from normal incidence, we can reduce pulse spreading in larger spheres by restricting returns over a smaller range of incidence angles through the use of hollow or recessed solid retros.

Satellite Cross-Section

For a spherical satellite, the nominal array cross-section is given by [Degnan, 1993]

$$\sigma = \frac{\sigma_{cc} N}{2}\left[1 - \frac{\sin^2\left(\frac{\theta_{\max}}{2}\right)}{\left(\frac{\theta_{\max}}{2}\right)^2}\right] = \frac{\sigma_{cc}}{2}\frac{\beta 4\pi R_s^2}{A_{cc}}\left[1 - \frac{\sin^2\left(\frac{\theta_{\max}}{2}\right)}{\left(\frac{\theta_{\max}}{2}\right)^2}\right]$$

where θ_{max} is the maximum acceptance angle of the cube corner, σ_{cc} is the optical cross-section of a single cube corner at normal incidence, N is the total number of retroreflectors on the spherical satellite, A_{cc} is the surface area occupied by a cube corner, R_s is the satellite radius, and β is the retro "packing density". The maximum acceptance angle θ_{max} can be expressed as a function of the time spread Δt and the satellite radius, i.e.

$$\theta_{\max} \cong \sqrt{\frac{c\Delta t}{R_s - nL\left(1 + 1/n^2\right)}}$$

From the bottom graph, a 70 cm radius Super-LAGEOS with the same cross-section and a 100 psec total spread is feasible. Retros would be recessed such that θ_{max} = 11.9º, and the satellite would be heavier to counteract the increased drag.

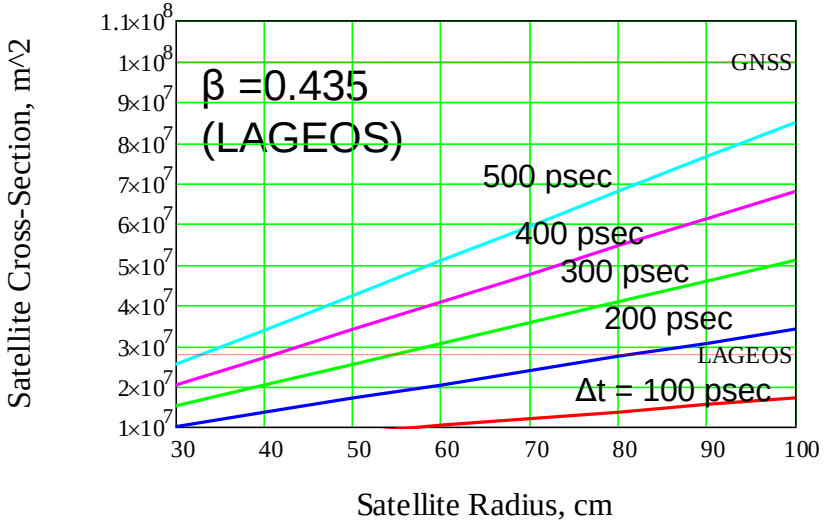

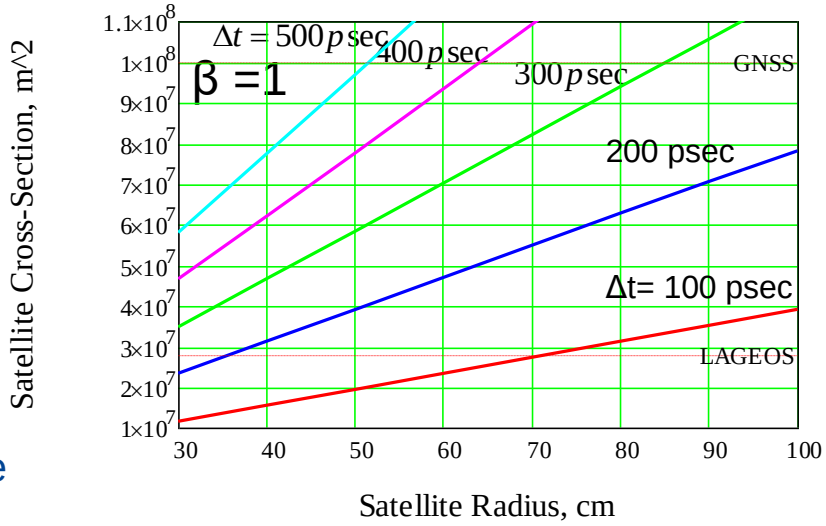

GNSS and Geostationary Satellites

Challenges: GNSS and Geosynchronous Satellites have the following characteristics:

1. Their orbital altitudes correspond to several Earth radii
2. They generally perform a utilitarian function (Earth observation, communications, navigation, etc.) which keeps the nadir side of the satellite approximately facing the Earth CoM.
3. The velocity aberration α is typically in the range 20 to 25 μrad and the variation is very small.
4. For a maximum zenith tracking angle of 70^o, beam Incidence angles can vary from 0 to θ_{lim} where

$$\theta_{\lim} = a\sin\left[\frac{R_E}{R_E + h}\sin(110^0)\right]$$

=13.1 deg for GNSS satellites at 20,000 km
= 8.2 deg for GEO satellites at 36,000 km

The smaller range of incidence angles implies limited pulse spreading from a flat array, especially if the array is compact in size and the retros are densely packed together to achieve the necessary cross-section. Nevertheless, the maximum flat panel induced spreading due to zenith tracking angle is still 474 psec (7 cm) and 292 psec (4.4 cm) per linear foot of array for GNSS and GEO satellites respectively. This spreading can increase further if satellite attitude deviations from true nadir extend the range of incidence angles. Furthermore, the impulse response varies with satellite elevation and azimuthal angle.

Solution: Flat panels can be replaced by a segment of a large sphere that simultaneously provides roughly the same desired cross-section (10^8 m^2) and the same amount of pulse spreading from all view angles.

GNSS Array Characteristics

If we replaced the current flat panels on GNSS satellites with a segment of a sphere with radius R_s, the minimum radius of the array footprint on the nadir-viewing side of the satellite would be given by

$$R_A = R_S \tan(\theta_{\max} + \theta_{\lim})$$

where we have assumed standard 38 mm diameter retros, a fill factor β ~0.8, θ_{lim} = 13.1° for GNSS satellites and used the following equation

$$\theta_{\max} \cong \sqrt{\frac{c\Delta t}{R_s - nL\left(1+1/n^2\right)}}$$

and assumed the ILRS recommended GNSS cross-section of 10^8 m^2 to generate the following graphs

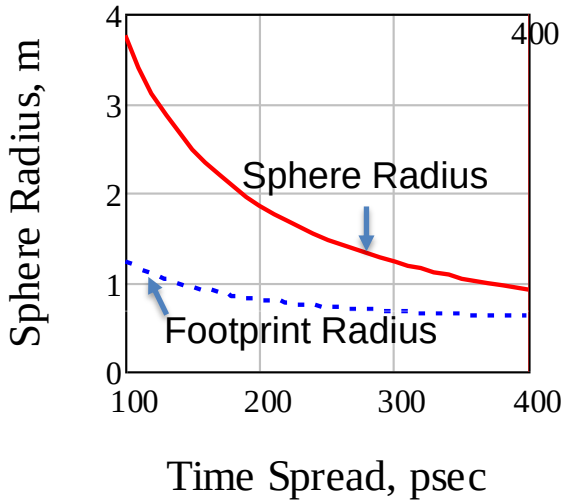

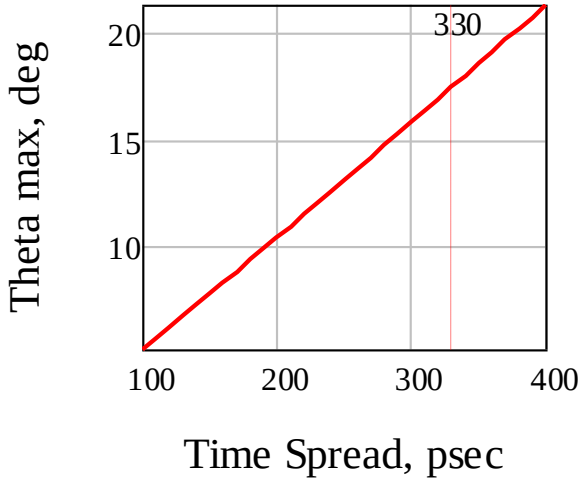

GNSS Retroreflector Size

The results on the last slide assumed a standard 38 mm diameter retroreflector and resulted in a rather large footprint (1 to 2 m) on the nadir-viewing face of the spacecraft. However, because the range of velocity aberration is rather narrow for GNSS and higher satellites, one has the option of using a larger retroreflector. Since the optical cross-section increases as D^4 power but the occupied area increases only as D^2, one can envision a smaller sphere with fewer retros embedded into it and therefore a smaller footprint. A cursory analysis suggests that retro diameters up to 64 mm can be used, yielding the following results for a fill factor of $\beta = 0.8$.

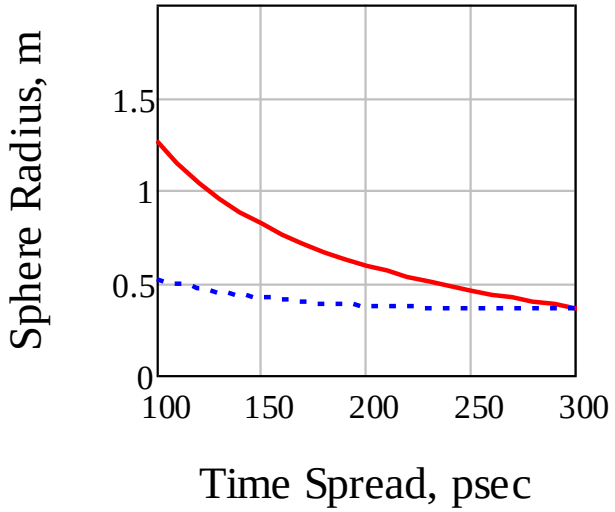

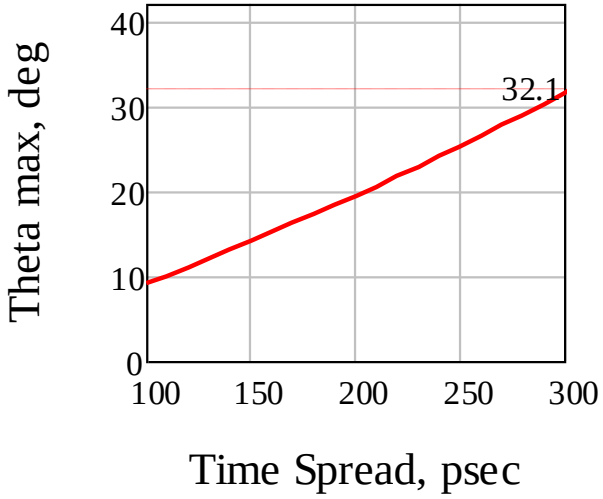

Summary

- **We have proposed both a theoretical and an experimental method for correcting the range bias in a normal point for an arbitrary return rate**.
- **This method not only provides a potentially bias-free range measurement but also removes the restriction to use only low return rates** thereby greatly
  - Reducing the integration time for normal point generation and reducing the length of the orbital path which defines that normal point.
  - Enhancing satellite data volumetric output in kHz SLR systems
  - Speeding up the interleaving of satellites.
- The **theoretical method** determines the function λ(t) by convolving the "known" PDFs for the laser, target, and receiver and then uses the result to compute the various PDFs associated with higher values of n and their corresponding time or range centroids, t_n.
- The **experimental method** uses low return rate measurements(<10%) to a particular target (calibration or satellite) to determine the single pe PDF $P_1(t)$ for that target and again uses that result to compute the PDFs and centroids for higher values of n. High frequency noise in the experimental data can be removed by a smoothing method, e.g. computing the Fourier transform, applying a bandwidth filter, and performing an inverse Fourier Transform.
- **The PDF approach assumes that the target response is largely independent of viewing angle,** as with uniformly populated spherical geodetic satellites (LAGEOS, Starlette, etc.) or remote sensing or GNSS satellites where legacy flat panel arrays are replaced by segments of uniformly populated spheres.
- Our results to date using NGSLR data suggest that the range bias is expected to vary linearly from 0 at very low return rates to a maximum on the order of -27 mm at very high return rates near 100%. **Thus, two bias measurements at a very low and very high rate can define the bias at all rates.**

ACKNOWLEDGEMENT. The author wishes to thank Dr. Michael Pearlman of the Smithsonian Astrophysical Observatory (SAO) for sponsoring my travel to the Stuttgart Workshop under his NASA grant.